IEEE Access
Multidisciplinary | Rapid Review | Open Access Journal

Received March 21, 2018, accepted April 24, 2018, date of publication April 30, 2018, date of current version June 5, 2018.

*Digital Object Identifier 10.1109/ACCESS.2018.2831218*

# A Novel Cognitive Satellite Network With GEO and LEO Broadband Systems in the Downlink Case

**CHUANG WANG[1], DONGMING BIAN[1], SHENGCHAO SHI[1], JUN XU[1], AND GENGXIN ZHANG[2]**

[1]College of Communications Engineering, Army Engineering University of PLA, Nanjing 210007,China
[2]Nanjing University of Posts and Telecommunications, Nanjing 210003, China

Corresponding author: Dongming Bian (biandm_satlab@163.com)

This work was supported by the National Natural Science Foundation of China under Grant 91338201, Grant 91738201, and Grant 91438109.

**ABSTRACT** With the development of satellite communication, the number of satellites in space continuously increases. However, the available spectrum resources are scarce. To address the spectrum scarcity, sharing the spectrum between different communication systems is a promising option. In this paper, a novel cognitive satellite network with geostationary earth orbit (GEO) and low earth orbit (LEO) broadband systems is studied in the downlink case. First, we present a general interference analysis model and simplify it by transforming the spatial dimension into the time dimension according to the satellite motion. Based on the interference analysis, an optimization algorithm with beamhopping and adaptive power control techniques is proposed, which can simultaneously enhance the spectral efficiency and protect the primary system. The system performance of the coexistence scenario is evaluated in terms of the system throughput. Numerical results demonstrate that the spectrum-sharing method between GEO and LEO systems is feasible, and the cognitive network can achieve a high spectral efficiency. Furthermore, the factors that affect the system in the spectral coexistence scenario are analyzed.

**INDEX TERMS** Cognitive satellite network, broadband satellite communication, dual satellite coexistence, beamhopping, adaptive power control.

## I. INTRODUCTION

With the rapid development of information society, the demand for ubiquitous and high-quality service continuously increases worldwide. Increasingly many satellites have been or will be launched into space to satisfy the growing demand, especially the recent surge of announcements concerning the mega-constellation satellite networks composed of hundreds of satellites, such as SpaceX, OneWeb and LeoSat [1]–[3]. However, the available radio spectrum resource is scarce, which is a bottleneck for the satellite system development. Currently, the spectrum resource is mainly allocated and coordinated by the International Telecommunication Union (ITU) according to the service regions and types. For example, L and S bands for mobile service have been fully allocated, and Ku and Ka bands for broadband service are depleting [4].

The concept of cognitive radio was first proposed by Mitola [5] and is widely applied in various fields, e.g., Internet of things [6], cellular mobile communication [7], WiMAX [8], wireless sensor network [9], aeronautical communication [10], ad hoc network [11] and satellite communication [12]. Although cognitive radio in terrestrial wireless systems has been deeply studied and evaluated in tests, the usage in satellite communications faces new challenges, e.g., system architecture, propagation model, round-trip delay, receiver characteristics, satellite characteristics, wide beam coverage, power level and limited possibilities of evolution due to the long system development and the fixed design space segment [13], [14]. In addition, many cognitive technologies are adopted for spectrum sharing, e.g., spectrum sensing [15]–[18], smart antennas and beamforming [19]–[21], shielding [22], beacon signaling [18], [23], interference alignment [24]–[26], precoding [27], power control [14], [28]–[30], beamhopping [31], [32] and network coding [33].

Research on cognitive satellite scenarios can be categorized into cognitive hybrid networks and dual satellite networks, where the spectrum is shared between a satellite

system and a terrestrial system and between two satellite systems, respectively. In a hybrid network, the satellite system can be considered the primary user, whereas the terrestrial system acts as the secondary user [22], [34], [35] and vice versa [19], [28], [30], [36]. For example, a satellite system serves as an auxiliary to connect the terrestrial base stations, where the terrestrial system and satellite uplink share the same spectrum [36]. In a dual satellite network, two satellite systems operate simultaneously over a coverage area in the same spectrum band. The cognitive radio is introduced to achieve different goals, such as spectrum utilization improvement [15], [37], [38] and channel availability improvement [39], [40].

However, most studies focused on static scenarios, where the satellites are almost Geostationary Earth Orbit (GEO) satellites. For Non-GeoStationary Orbit (NGSO) satellites, the system architecture will dynamically change. If an NGSO system coexists with another satellite system, it is very likely to produce in-line interference when the satellites and users from different systems are in alignment, which will make the systems paralyzed. The importance of finding applicable spectrum sharing possibilities between GEO and NGSO systems is rapidly increasing due to the foreseen mega-constellation concepts.

To address the challenge, [41] proposes an analytical method for assessing interference between satellite systems, and the effect of NGSO interference on the bit error rate of a GEO system is studied in [42]. The ITU presents some recommendations for spectrum sharing, including limit on equivalent power flux density, satellite diversity and alternate polarization [43]. Reference [29] proposes an adaptive power control technique for the coexistence scenario of GEO and NGSO satellites. Reference [14] points out that awareness of other systems' operational characteristics, such as frequency allocations, orbital positions, and antenna patterns, is a key for a successful coexistence between satellite systems in the same band. Moreover, it analyzes the feasibility of spectrum sharing between GEO and NGSO systems through a database approach. In practical terms, O3b and OneWeb systems operate in the Ku and Ka bands, respectively, and share part of the same frequency with the GEO satellite [2], [44]. In addition, the OneWeb system introduces an innovative technique, i.e., progressive pitch, which avoids interference by gradually and slightly tilting the satellite as it approaches the equator to ensure that it does not cause or receive interference.

There have been some breakthroughs in the study of spectrum sharing between GEO and NGSO systems. However the studied scenarios are relatively simple with mostly one satellite, one beam and one user in one system. More research especially on dynamic sharing approaches is required. Additionally, the GEO system is always considered a primary system, whereas the NGSO system is set as a secondary system in previously studied cognitive networks. Nevertheless, there are several frequency bands which permit NGSO operations on an exclusive primary basis. Specifically, the 18.8-19.3 GHz band allocated to the LeoSat system is a typical case. Accordingly to [3, Sec. 6.1.2], LeoSat's proposed operations in the 18.8-19.3 GHz downlink band are not subject to ITU EPFD limits, and are consistent with the FCC's Ka-band plan, which permit NGSO operations on an exclusive primary basis [45].

In this paper, we propose a novel spectrum-sharing method between GEO and Low Earth Orbit (LEO) satellite systems based on beamhopping and adaptive power control techniques. The LEO satellite constellation acts as the primary system, whereas the GEO satellite serves as the secondary system. With the information sharing of satellite ephemeris between the GEO system and the LEO system, the dynamic interference can be effectively mitigated. Specifically, beamhopping and adaptive power control techniques are used at the secondary system to enhance spectral efficiency and ensure the coexistence without disruption.

The remainder of this paper is organized as follows. In Section II, the model of interference analysis is discussed. The configuration of the cognitive satellite network with GEO and LEO satellites is proposed in Section III. Section IV presents the algorithm with beamhopping and adaptive power control techniques, and numerical analysis is conducted with simulations. Section V concludes the paper.

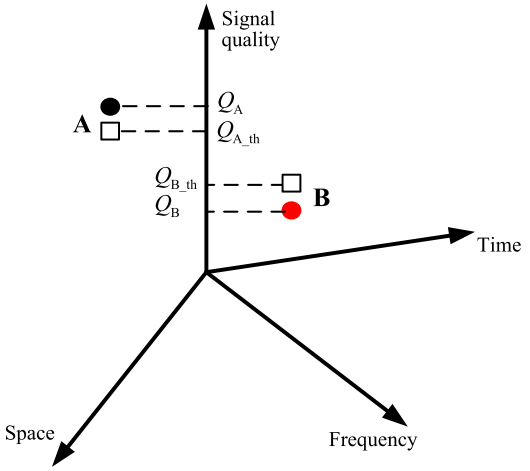


**FIGURE 1.** Schematic diagram of node coexistence in the network.

## II. INTERFERENCE ANALYSIS MODEL

For a network with many nodes, the necessary condition that an entire network normally operates without disruption can be summarized as follows: the quality of the signal, i.e., Carrier to Interference plus Noise Ratio (CINR)[1] received by each node must exceed the threshold required for normal operation. Only under this condition can multiple nodes coexist in the network. As shown in Fig. 1, node A at a certain position receives a signal of a certain frequency at a certain time.

[1] There are many similar indicators to measure the signal quality [46], such as $C/(n_0 + I_0)$, $C/(N + I)$ and $C/(T_n + T_I)$. We define the CINR as the signal quality indicator, which is equal to the Signal to Interference plus Noise Ratio (SINR) in this work.

The signal quality is greater than the required threshold, so node A can work normally. For node B, the signal quality is less than the threshold, so node B cannot properly work.

To make the entire network normally operate, we prefer the situation of node A and avoid that of B when we design a network. Since the signal is distributed over three dimensions (space, time and frequency), the interference can be directly avoided by the distinction of dimensions. Specifically, it can be achieved using a time slot division in the time dimension, position isolation in the space dimension and spectrum differentiation in the frequency dimension, as shown in Fig. 2.

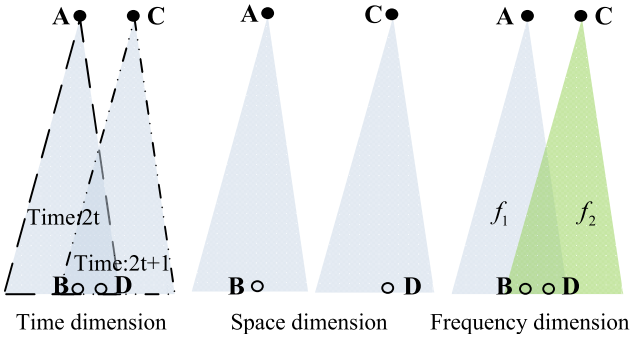


**FIGURE 2.** Interference avoided by the distinction of dimensions.

If the interference cannot be avoided through the distinction of dimensions, the signal quality should be estimated whether the node can operate normally. As shown in Fig. 3, many nodes use the identical frequency to simultaneously communicate. Since the distinction of dimensions cannot be achieved, the nodes interfere with each other. Nevertheless, the coexistence of multiple nodes can be achieved when the signal quality of each node satisfies the requirement.

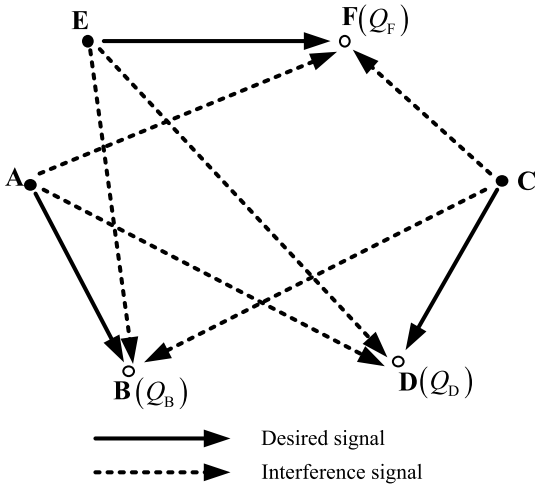


**FIGURE 3.** Coexistence of multiple nodes at a certain time with identical frequency.

The proposed idea of node coexistence can be expressed as the corresponding mathematical model:

$$\forall t \in T, s \in S, f \in F, \quad \text{s.t.} \ \frac{C}{N+I}(t,s,f) \geq \left(\frac{C}{N+I}\right)_{\text{th}}(t,s,f) \tag{1}$$

where $T$ represents the duration of the network; $S$ represents the position of all nodes; $F$ represents all frequencies in the network; $\frac{C}{N+I}(t,s,f)$ denotes the signal quality of a node at $s$, which operates with frequency $f$ at time $t$. The above expression indicates that the signal quality of all nodes with any frequency in the network should exceed the threshold at every moment. Only in this case can the entire network properly operate.

The satellite motion conforms to Kepler's Three Laws, and the satellite's trajectory can be equivalent to a collection of infinite positions. Therefore, if only the satellite orbit is settled, the coordinate of the satellite's position is time-dependent. The common orbital parameters in two-body motion is semimajor axis $a$, eccentricity $e$, inclination angle $i$, right ascension of the ascending node $\Omega$, argument of perigee $\omega$ and time past perigee $t_p$. Reference [47] provides the method to compute the position vector of a satellite in the Earth-Centered Earth-Fixed (ECEF) coordinate system from the orbital parameters. Accordingly, if the satellite orbital parameters are determined, the position coordinate in motion is a function of time as shown in Equation (2).

$$s(x,y,z) = \Phi(t) \tag{2}$$

Then, variable $s$ in (1) can be replaced by $t$. Specifically, every satellite should follow the constraint:

$$\forall t \in T, f \in F, \quad \text{s.t.} \ \frac{C}{N+I}(t,f) \geq \left(\frac{C}{N+I}\right)_{\text{th}}(t,f) \tag{3}$$

In addition, if all satellites in the network use the identical frequency, the constraint condition for every satellite becomes (4). Therefore, the signal quality is only related to time, and the interference can be mitigated through management in the time dimension.

$$\forall t \in T, \quad \text{s.t.} \ \frac{C}{N+I}(t) \geq \left(\frac{C}{N+I}\right)_{\text{th}}(t) \tag{4}$$

Carrier power $C$ and noise power $N$ in the CINR can be calculated as follows:

$$C = \frac{EIRP \cdot G_R}{L_f} = \frac{P_T G_T G_R}{L_f} \tag{5}$$

$$N = kT_nB \tag{6}$$

where $EIRP$ represents the equivalent isotropic radiated power of the transmitter, $P_T$ represents the transmit power, $G_T$ represents the gain of the transmit antenna, $G_R$ represents the gain of the receive antenna, $L_f$ represents the free space propagation loss, $T_n$ represents the equivalent noise temperature of the receiver, $B$ represents the transponder bandwidth, and $k$ is Boltzmann constant.

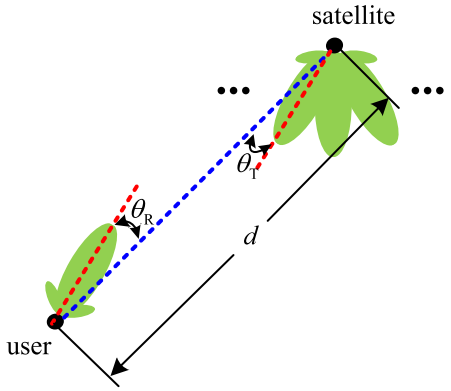


**FIGURE 4.** Off-boresight angle of the transmitter and receiver in the direction of the beam.

The antenna gain is related to the off-boresight angle of the transmitter or receiver in the beam direction, as shown in Fig. 4. The off-boresight angle can be calculated through the beam direction and the position vector of the satellite and user [47]. The angle varies when the satellite moves, which results in the dynamic of the gain. Particularly, the off-boresight angle of receiver $\theta_R$ for the desired user is 0 because the user's antenna continues tracking the satellite. The expression to calculate the gain of the antenna is [48]:

$$G = G_0\left[\frac{J_1(\mu)}{2\mu} + 36\frac{J_3(\mu)}{\mu^3}\right]^2 \tag{7}$$

where $\mu = 2.07123\sin(\theta)/\sin(\theta_{3dB})$; $J_1$ and $J_3$ are the first and third order Bessel functions, respectively; $\theta$ is the off-boresight angle; $\theta_{3dB}$ is the angle that corresponds to the 3dB beamwidth; $G_0$ is the maximum antenna gain when the off-boresight angle is 0, and its expression is:

$$G_0 = \eta\frac{4\pi A}{(c/f)^2} \tag{8}$$

where $A$ represents the antenna area, $\eta$ represents the antenna efficiency and c is the velocity of light. In addition, the free space propagation loss is a function of the distance between transmitter and receiver and it can be calculated by (9).[2]

$$L_f = \left(\frac{4\pi d}{c/f}\right)^2 \tag{9}$$

The interference signal may come from different sources with different intensity. Furthermore, the total interference power received by the terminal can be summarized as follows:

$$I = \sum_{m=1}^{M} V_m I_m \tag{10}$$

where $M$ represents quantity of interference transmitters in the network. $V_m$ is defined as the interference factor between the $m$-th interference source and the terminal, and its value is 0-1. Specifically, it is related to the visibility of the two nodes, orthogonality and bandwidth overlap between the signals. For example, if it is invisible, then $V_m = 0$. $I_m$ represents the received interference power from the $m$-th transmitter, and it can be calculated by interchanging the appropriate variables in (5). By substituting (5), (6) and (10), the CINR can be calculated as follows:

$$\frac{C}{N+I} = \frac{\frac{P_{T,0}G_{T,0}G_{R,0}}{L_0}}{\sum_{m=1}^{M}\left[V_m\cdot\frac{P_{T,m}G_{T,m}G_{R,m}}{L_m}\right] + kT_nB} \tag{11}$$

where T and R in the subscript denote the transmitter- and receiver-related variables, respectively; $m$ in the subscript represents the $m$-th interference source; 0 denotes the desired signal.

## III. CONFIGURATION OF THE COGNITIVE SATELLITE NETWORK

In this work, we propose a new cognitive satellite network with a GEO satellite and an LEO satellite constellation in the downlink case, as shown in Fig. 5. The LEO system is composed of a Ka-band LEO Walker constellation, in which the satellites have similar orbits, eccentricity and inclination, so that any perturbations affect each satellite in approximately the same way and the user on the ground can be serviced by different satellite periodically [49]. Additionally it serves as the primary system. The GEO satellite acts as the secondary system, which should coordinate to avoid disrupting the incumbent LEO system. In the cognitive satellite network, it is assumed that the gateways of both systems are connected by a high-speed loss-less fiber optic connection and exchange satellite ephemeris with each other.


**FIGURE 5.** Cognitive satellite network with the GEO and LEO satellite systems.

[2]The detailed calculation procedures of the aforementioned position coordinate, off-boresight angle and the distance $d$ are listed in the Appendix.

All LEO satellites deploy multibeam payloads with frequency reuse among the beams. The user's antenna always tracks the satellite, which implies that the antenna orientation dynamically changes. The secondary GEO satellite system is supposed to use a beamhopping payload. Specifically, we consider a time window with periodical time slots; in each time slot, only a subset of beams is illuminated. The user's antenna also continues tracking the GEO satellite. Beamhopping is an available, useful and efficient technique, particularly in high throughput satellites, because of many advantages, e.g., adaptability to dynamic and non-uniform distributed traffic demand, reduced number of on-board power amplifiers and fewer gateway stations required on the ground [50]. Moreover, the most notable feature is that a single wideband carrier occupies the entire bandwidth instead of several narrowband channels that intermingle in a transponder. Thus, the back-off of the amplifier and guard interval of the bandwidth can be avoided, and both power and bandwidth efficiency are improved. In this cognitive network, beamhopping has another advantage: the bandwidth overlaps between each LEO beam and GEO beam are identical and small, reciprocal of LEO's frequency reuse factor, the GEO user suffers a relatively weak interference caused by the LEO system, and each LEO user's interfered bandwidth caused by the GEO system is identical.

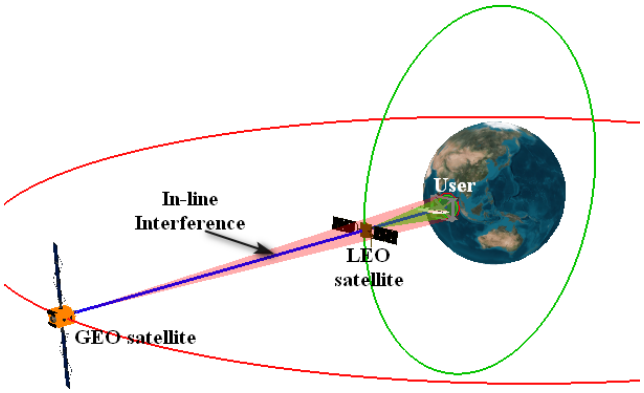


**FIGURE 6.** Schematic of in-line interference arising.

Since the LEO satellite moves relative to the ground, it is notably likely for the LEO satellite to fall into the line of sight between the GEO satellite and its ground terminal. Then, the in-line interference arises, and the signal quality rapidly decreases, which will make both systems paralyzed, as shown in Fig. 6. Nevertheless, when the network serves at high latitudes, the in-line interference scarcely occurs. Even near the equator, it only sustains a short time period. In a cognitive satellite network, the gateways between LEO and GEO satellites are connected, so that the channel state information and satellite ephemeris can be shared. Therefore, one can predict when and where the interference can occur. Then the GEO satellite can mitigate the interference in the time domain by reasonably allocating beams and decreasing the transmit power of the seriously disturbing beams.

## IV. COEXISTENCE SIMULATIONS

### A. INTERFERENCE ANALYSIS

The coverage of the GEO satellite is sufficiently large to reach one third of the earth, whereas the coverage of the LEO satellite is small and movable. A fixed area is consecutively served by LEO satellites. Therefore, when analyzing the interference between GEO and LEO systems in the downlink case, we focus on the interference in a designated region. Thus, a scenario of one GEO satellite and one LEO satellite is studied here as a representative. As shown in Fig. 7, the red beams marked with numbers are generated by a GEO satellite, and the others are generated by an LEO satellite. The frequency reuse factor of the LEO satellite is 7, where different colors represent the different frequencies. The GEO beams remain focused, whereas the LEO beams move with the satellite motion until the LEO satellite passes through and another comes. To simplify the analysis, the simulation is performed in the region covered by GEO beams, and the simulation time is set as the duration that one LEO satellite passes through the region. There is one GEO and LEO user in each GEO beam, and both are placed at the center of the beam. The satellite orbital parameters and simulation parameters are presented in Tables 1 and 2, respectively. The gain pattern of both GEO and LEO user's antenna is shown in Fig. 8 as a representative.

First, the interference between GEO and LEO satellites with all beams illuminated is simulated using Equation (11). Because the entire bandwidth is used in a GEO beam, each GEO user is interfered by multiple beams of LEO satellite during the simulation and vice versa for the LEO user.

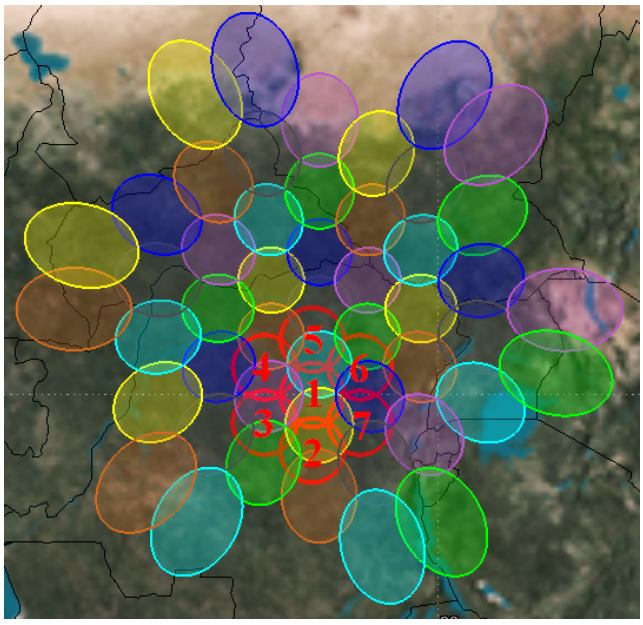


**FIGURE 7.** Distribution of multibeam for the GEO and LEO satellites.

**TABLE 1. Orbital Parameters of the GEO and LEO satellites.**

| Parameters | GEO | LEO |
|---|---|---|
| Semimajor axis | 42164.1 km | 7828.14 km |
| Eccentricity | 0 | 0 |
| Inclination angle | 0° | 90° |
| Right ascension of the ascending node | 57.4032° | 280.603° |
| Argument of perigee | 0° | 0° |
| Time past perigee | 0 s | 0 s |

**TABLE 2. Simulation parameters.**

| Parameters | Notations | Value |
|---|---|---|
| Frequency band | $f$ | 19 GHz (Ka) |
| Analysis start time | $t_{\mathrm{st}}$ | 24 8 2017 06:50:51 |
| Analysis stop time | $t_{\mathrm{sp}}$ | 24 8 2017 06:53:45 |
| Time step | $\Delta t$ | 1 s |
| Noise temperature of receive antenna | $T_{\mathrm{n}}$ | 290 K |
| Antenna efficiency | $\eta$ | 55% |
| Antenna diameter of GEO satellite | $D_{\mathrm{GS}}$ | 2.4 m |
| Antenna diameter of GEO user | $D_{\mathrm{GU}}$ | 0.3 m |
| Bandwidth of GEO beam | $B_{\mathrm{G}}$ | 200 MHz |
| Number of GEO beams | $N_{\mathrm{GB}}$ | 7 |
| Transmit power of GEO beam | $P_{\mathrm{GS}}$ | 300 W |
| Antenna diameter of LEO satellite | $D_{\mathrm{LS}}$ | 0.1 m |
| Antenna diameter of LEO user | $D_{\mathrm{LU}}$ | 0.3 m |
| Bandwidth of LEO beam | $B_{\mathrm{L}}$ | 25 MHz |
| Frequency reuse factor | $K$ | 7 |
| Number of LEO beams | $N_{\mathrm{LB}}$ | 37 |
| Transmit power of LEO beam | $P_{\mathrm{LS}}$ | 50 W |

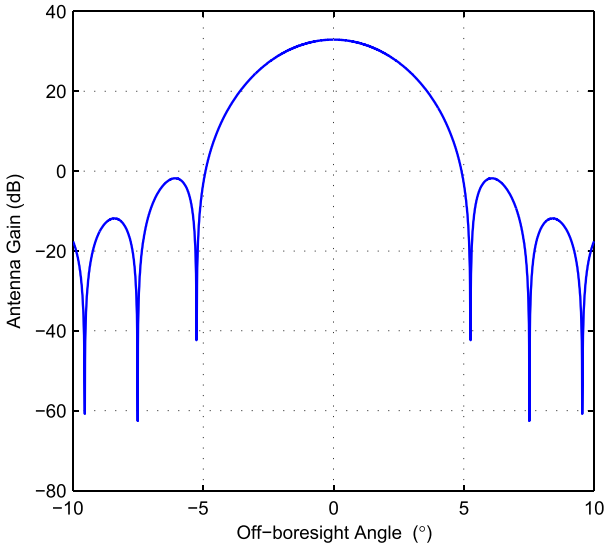


**FIGURE 8. Gain pattern of the user's antenna.**

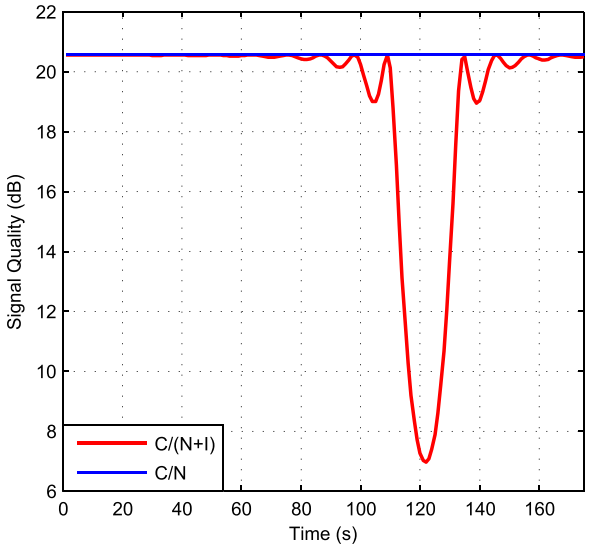


**FIGURE 9. Signal quality of the GEO user in the No. 2 beam.**

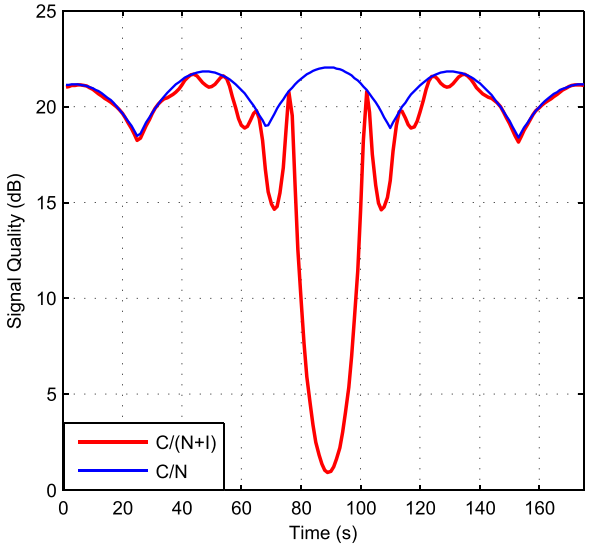


**FIGURE 10. Signal quality of the LEO user in the No. 1 beam.**

Fig. 9 shows the signal quality values of a GEO user in beam No. 2 during the simulation, where the blue curve represents the original signal, and the red curve represents the signal interfered by the LEO satellite. Fig. 10 shows the variation of signal quality for the LEO user in beam No. 1.

For the GEO system, the desired signal that is transmitted from the GEO satellite is almost unchanged, which results in a blue curve in Fig. 9. However, the interference signal transmitted from the LEO satellite varies with the motion of the LEO satellite. Thus, the quality of the interfered signal in Fig. 9 deteriorates for a moment. For the LEO system, the desired signal transmitted from the LEO satellite periodically varies as the beams pass through one by one. Because the antenna of the LEO user always tracks the LEO satellite during the satellite passage, the interference signal transmitted from the GEO satellite varies as shown in the red curve in Fig. 10. Because of the limited space, only one user's simulation of each satellite is shown. The signal quality of other satellites similarly varies.

### B. ALGORITHM FOR BEAMHOPPING SYSTEM

Based on the above analysis, we can infer that during the passage of the LEO satellite, interference arises and affects both systems. In addition, the interference is short-lived and predictable. Moreover, the interference effects caused by different GEO beams are staggered in time. For example,

No. 1 GEO beam seriously disturbs the LEO user in the middle of the simulation time, but other beams generate little interference at the same time. Therefore, if the GEO and LEO system reasonably coordinate, there is a substantial possibility for them to coexist in the downlink.

In particular, GEO users are always interfered by all beams from the LEO satellite, whereas LEO users are only interfered by the illuminated beams in each time slot. To reduce the effect on harmful interference, the beamhopping sequence of the GEO satellite should be optimally designed. First, the signal quality of the GEO users that are interfered by all LEO beams and the signal quality of LEO users that are interfered by each GEO beam is calculated based on the satellite ephemeris and (11). Let $\Upsilon_{\mathrm{GEO},n,j}$ indicate the SINR of the $n$-th GEO user in the $j$-th time slot, and $\Upsilon_{\mathrm{LEO},u,i,j}$ is the SINR of the $u$-th LEO user interfered by the $i$-th GEO beam in the $j$-th time slot. The variation of $\Upsilon_{\mathrm{GEO},n,j}$ during the simulation time is shown in Fig. 11. The variation of $\Upsilon_{\mathrm{LEO},u,i,j}$ when $i = 1$ is shown in Fig. 12.

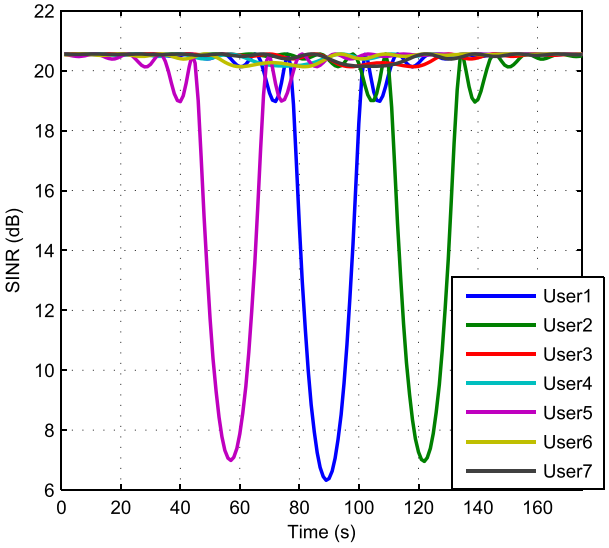


**FIGURE 11.** SINR of the GEO users with all GEO and LEO beams illuminated.

As the secondary system, the GEO system must ensure that the interference that it causes is beyond the threshold of the LEO system. A regular time window is periodically applied for the beamhopping GEO system. In each time slot, the entire bandwidth is allocated to the illuminated beams. We consider $N_{\mathrm{T}}$ to be the number of time slots in each time window, and $N_{\mathrm{GB}}$ is the number of beams in the GEO system. Thus, the $N_{\mathrm{T}} \times N_{\mathrm{GB}}$ beam illumination matrix T can be written as:

$$T = \begin{bmatrix} T_{11} & T_{21} & \cdots & T_{N_{\mathrm{GB}}1} \\ T_{12} & T_{22} & \cdots & T_{N_{\mathrm{GB}}2} \\ \vdots & \vdots & \ddots & \vdots \\ T_{1N_{\mathrm{T}}} & T_{2N_{\mathrm{T}}} & \cdots & T_{N_{\mathrm{GB}}N_{\mathrm{T}}} \end{bmatrix} \tag{12}$$

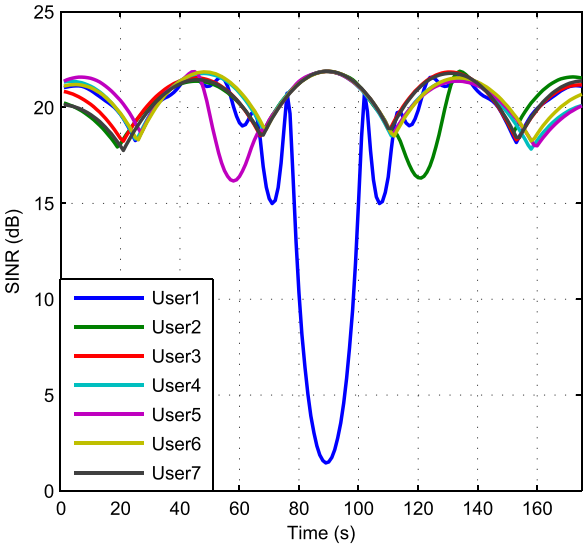


**FIGURE 12.** SINR of the LEO users with GEO No. 1 beam and all LEO beams illuminated.

where $T_{ij}$ denotes whether the $i$-th beam in the $j$-th time slot is illuminated. Its value is 1 when illuminated and 0 otherwise. The total number of time slots allocated to the $i$-th beam in a time window can be calculated as: $N_{i,\mathrm{T}} = \sum_{j=1}^{N_{\mathrm{T}}} T_{ij}$, and the total number of beams illuminated in the $j$-th time slot is: $N_{\mathrm{B},j} = \sum_{i=1}^{N_{\mathrm{GB}}} T_{ij}$.

The beamhopping technique can mitigate the interference to some extent. However, there is inevitably harmful interference when considering fairness in the distribution among the beams. To compensate for the shortcoming, the adaptive power control technique is used. By decreasing the transmit power of the inevitably illuminated GEO beam, the constraint of the LEO system is satisfied. For convenience, the time window $N_{\mathrm{T}}$ is set to be identical to the number of GEO satellite beams, which implies that only one beam is illuminated in each time slot, and every beam must be illuminated in a time window for the purpose of fairness. In this work, we consider the maximum throughput of cognitive network to be the objective. To maximize the total system throughput based on the node coexistence idea proposed in (4) and fairness among the beams, the following optimization problem is formulated:

$$\begin{aligned} &\max \ \Re_{\mathrm{GEO}} + \Re_{\mathrm{LEO}} \\ &\text{s.t.} \begin{cases} \Upsilon_{\mathrm{LEO},u,j} \geq \Upsilon_{\mathrm{th}} & (u = 1, \ldots, N_{\mathrm{LU}}; j = 1, \ldots, N_{\mathrm{T}}) \\ N_{i,\mathrm{T}} = 1 & (i = 1, \ldots, N_{\mathrm{GB}}) \end{cases} \end{aligned} \tag{13}$$

where $\Re_{\mathrm{GEO}}$ and $\Re_{\mathrm{LEO}}$ represent the system throughput of the GEO and LEO, respectively, and $\Upsilon_{\mathrm{LEO},u,j}$ represents the SINR of the $u$-th LEO user in the $j$-th time slot.

The expressions are described as follows:

$$\begin{aligned}
\Re_{\mathrm{GEO}} &= \frac{B_{\mathrm{G}}}{N_{\mathrm{GU}}} \sum_{i=1}^{N_{\mathrm{GB}}} \sum_{j=1}^{N_{\mathrm{T}}} \sum_{n=1}^{N_{\mathrm{GU}}} \log_2\left(1 + T_{ij} \cdot \Upsilon_{\mathrm{GEO},n,j}\right) \\
\Re_{\mathrm{LEO}} &= \frac{B_{\mathrm{L}} N_{\mathrm{LB}}}{N_{\mathrm{LU}} N_{\mathrm{T}}} \sum_{j=1}^{N_{\mathrm{T}}} \sum_{u=1}^{N_{\mathrm{LU}}} \log_2\left(1 + \Upsilon_{\mathrm{LEO},u,j}\right) \\
\Upsilon_{\mathrm{GEO},n,j} &= \frac{\frac{P_{\mathrm{GS},n,j} G_{\mathrm{GS-GU},n,j} G_{\mathrm{GU-GS},n,j}}{L_{\mathrm{GS-GU},n,j}}}{\sum_{h=1}^{N_{\mathrm{LB}}} \left[\tau_{\mathrm{G}} \cdot \frac{P_{\mathrm{LS},h,j} G_{\mathrm{LS-GU},n,h,j} G_{\mathrm{GU-LS},n,h,j}}{L_{\mathrm{LS-GU},n,j}}\right] + k T_{\mathrm{n}} B_{\mathrm{G}}} \\
\Upsilon_{\mathrm{LEO},u,j} &= \sum_{i=1}^{N_{\mathrm{GB}}} T_{ij} \cdot \Upsilon_{\mathrm{LEO},u,i,j} \\
\Upsilon_{\mathrm{LEO},u,i,j} &= \frac{\frac{P_{\mathrm{LS},u,j} G_{\mathrm{LS-LU},u,j} G_{\mathrm{LU-LS},u,j}}{L_{\mathrm{LS-LU},u,j}}}{\tau_{\mathrm{L}} \frac{P_{\mathrm{GS},i,j} G_{\mathrm{GS-LU},u,i,j} G_{\mathrm{LU-GS},u,i,j}}{L_{\mathrm{GS-LU},u,j}} + k T_{\mathrm{n}} B_{\mathrm{L}}} \\
&\quad (n = 1, \ldots, N_{\mathrm{GU}}) \\
&\quad (h = 1, \ldots, N_{\mathrm{LB}})
\end{aligned} \tag{14}$$

where $\tau$ represents the bandwidth overlap of the interference signal. $\tau_{\mathrm{G}} = 0.125$ for the GEO system, and $\tau_{\mathrm{L}} = 1$ for the LEO system. The interpretation of some variables in (14) are presented in Table 3. The meanings of the other variables can be deduced by interchanging the corresponding subscript. It should be pointed out that the users are covered by one GEO and LEO beam in each time slot, so there is a one-to-one correspondence between the users and the beams for the desired signal. Therefore, the subscript of the beam in some variables is omitted for convenience.

The system throughput is positively correlated with the signal quality. Thus, the objective function can be transferred to the maximum SINR. To simply solve the optimization problem, we propose Algorithm 1.

**TABLE 3. Interpretation of some variables in (14).**

| Notations | Meaning |
|---|---|
| $P_{\mathrm{GS},n,j}$ | Transmit power of GEO satellite for the $n$-th GEO user in the $j$-th time slot |
| $P_{\mathrm{LS},h,j}$ | Transmit power of LEO satellite's $h$-th beam in the $j$-th time slot |
| $G_{\mathrm{GS-GU},n,j}$ | Gain of GEO satellite's antenna from direction of the $n$-th GEO user in the $j$-th time slot |
| $G_{\mathrm{LS-GU},n,h,j}$ | Gain of LEO satellite's $h$-th beam from direction of the $n$-th GEO user in the $j$-th time slot |
| $L_{\mathrm{GS-GU},n,j}$ | Free space propagation loss from the GEO satellite to the $n$-th GEO user in the $j$-th time slot |

In Algorithm 1, function $\min_x(A)$ means finding the suitable value of $x$ to acquire the minimum $A$. And function $\max_x(A)$ works oppositely from $\min_x(A)$. According to the algorithm, the simulation time is divided into cycles by the length of the time window, and the beamhopping sequence is optimized in each time window. To satisfy the interference

**Algorithm 1** Optimization Algorithm With Beamhopping and Adaptive Power Control

**Input:** $\Upsilon_{\mathrm{GEO},i,j}, \Upsilon_{\mathrm{LEO},u,i,j}, N_{\mathrm{T}}, \Upsilon_{\mathrm{th}}, N_{win}$
**Output:** $D_{\mathrm{T}}, D_{\mathrm{B}}$
**Begin:**
  **for** $a = 1$ to $N_{win}$ **do**
    $\left[\Upsilon_{\mathrm{LEO\_min}\,U}, I_{\mathrm{LEO\_min}\,U}\right] = \min_u\left(\Upsilon_{\mathrm{LEO},u,i,j} \,|\, j \in ((a-1)N_{\mathrm{T}}, aN_{\mathrm{T}}]\right)$
    **for** $b = 1$ to $N_{\mathrm{T}}$ **do**
      $\left[\Upsilon_{\mathrm{LEO\_max}\,T\_\mathrm{min}\,U}, I_{\mathrm{LEO\_max}\,T\_\mathrm{min}\,U}\right] = \max_j \Upsilon_{\mathrm{LEO\_min}\,U}$;
      $\left[\Upsilon_{\mathrm{LEO\_minB\_max}\,T\_\mathrm{min}\,U}, I_{\mathrm{LEO\_minB\_max}\,T\_\mathrm{min}\,U}\right] = \min_i \Upsilon_{\mathrm{LEO\_max}\,T\_\mathrm{min}\,U}$;
      $\left[\Upsilon_{\mathrm{GEO\_maxB\_max}\,T}, I_{\mathrm{GEO\_maxB\_max}\,T}\right] = \max_i \Upsilon_{\mathrm{GEO\_max}\,T}$
      **if** $\Upsilon_{\mathrm{LEO\_minB\_max}\,T\_\mathrm{min}\,U} > \Upsilon_{\mathrm{th}}$ & $\Upsilon_{\mathrm{LEO\_min}\,U}\Big|_{j = I_{\mathrm{GEO\_max}\,T}}^{i = I_{\mathrm{GEO\_maxB\_max}\,T}} > \Upsilon_{\mathrm{th}}$ **then**
        $D_{\mathrm{T}} = I_{\mathrm{GEO\_max}\,T}$;
        $D_{\mathrm{B}} = I_{\mathrm{GEO\_maxB\_max}\,T}$
      **else**
        $D_{\mathrm{T}} = I_{\mathrm{LEO\_max}\,T\_\mathrm{min}\,U}$;
        $D_{\mathrm{B}} = I_{\mathrm{LEO\_minB\_max}\,T\_\mathrm{min}\,U}$
        **if** $\Upsilon_{\mathrm{LEO\_minB\_max}\,T\_\mathrm{min}\,U} < \Upsilon_{\mathrm{th}}$ **then**
          Decrease the power of $D_{\mathrm{B}}$-th GEO beam in $D_{\mathrm{T}}$-th time slot
        **end if**
        $\Upsilon_{\mathrm{LEO},u,i,j}\Big|_{j = D_{\mathrm{T}}}^{u = I_{\mathrm{LEO\_min}\,U},\, i = D_{\mathrm{B}}} = \mathrm{Null}$
        $\Upsilon_{\mathrm{GEO},i,j}\Big|_{j = D_{\mathrm{T}}}^{i = D_{\mathrm{B}}} = \mathrm{Null}$
      **end if**
    **end for**
  **end for**
  **Return:** $D_{\mathrm{T}}, D_{\mathrm{B}}$

constraint, the worst signal quality of the LEO user must be greater than threshold. On one hand, we should select the beam and time slot that result in the maximum SINR of GEO user at first, on the other, the selected beam and time slot should let the worst LEO user exceed the threshold. If so, the corresponding beam and time slot are confirmed. If not, the beam that corresponds to the minimum SINR of the LEO user is selected, in case the user's signal quality is worse. Nevertheless, if the user's signal quality is still below threshold, the transmit power of the corresponding GEO beam should be decreased until the worst LEO user exceeds the threshold. Then, a beam and a time slot are decided, and the corresponding $\Upsilon_{\mathrm{GEO},i,j}$ and $\Upsilon_{\mathrm{LEO},u,i,j}$ should be updated. The next beam and time slot should be selected until the entire time window is completed. Then, the optimization continues until all time windows are completed. Here, $\Upsilon_{\mathrm{th}}$ is set to be 16 dB.

Fig. 13 shows the variation of the SINR during simulation, where the blue curves represent the SINR of all LEO users, and the red curve represents the SINR of the GEO users. Because of the beamhopping technique, only the illuminated

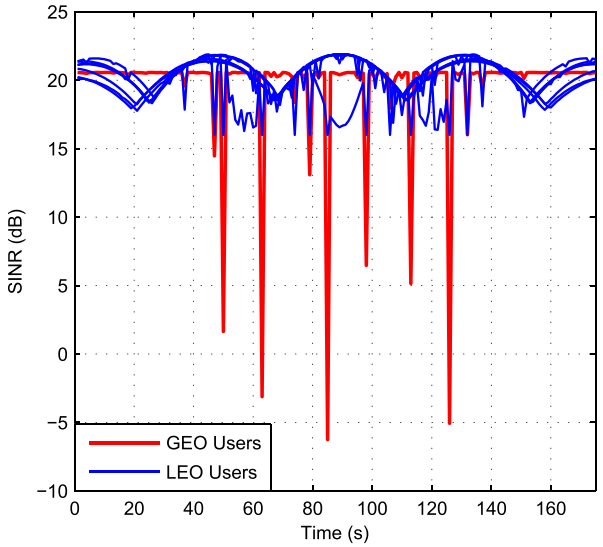


**FIGURE 13.** SINR of 7 LEO users and active GEO users.

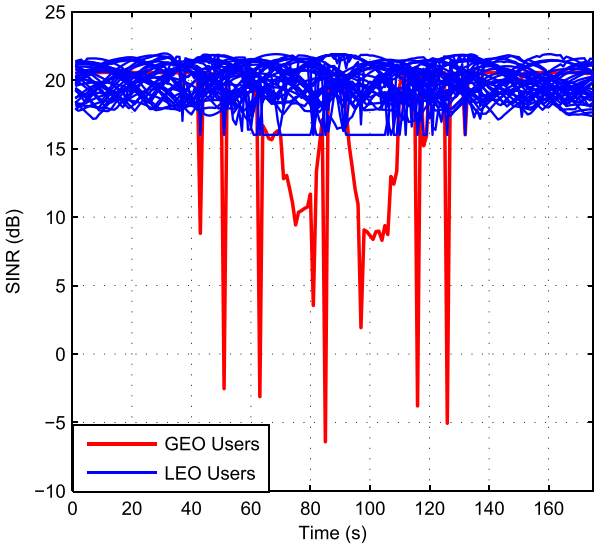


**FIGURE 14.** SINR of the users (5 LEO users in each beam).

GEO beam in every time slot is active. Thus, the blue curves are affected by different GEO beams, and the red curve is an assembly of SINR from different GEO users. The simulation shows that the interference is effectively mitigated. In addition, all LEO users satisfy the constraint, whereas the SINR of GEO users is notably low in a few time slots. The deterioration in the SINR of GEO users comes from the fact that the in-line interference lasts longer than the time window of beamhopping. Therefore, there are certain moments that strong interference is inevitable when only the beamhopping technique is adopted. Moreover, the deterioration caused by the interference occurs at the same time for GEO and LEO users. To protect the LEO system, the transmit power of the corresponding GEO beam should be decreased, which makes the signal quality of GEO user much worse.

When the traffic of the GEO system is delay-tolerate, the time window can be expanded to avoid the deterioration. The in-line interference can be completely avoided by illuminating the GEO beams in reasonable time slot. When the traffic of the GEO system is delay-sensitive, some promising candidates are envisaged to deal with this event: 1) Employing Adaptive Coding Modulation (ACM) technique [51]. 2) Increasing the size of the LEO user's antenna. 3) Using spread spectrum signals [52].

### C. EFFECT ON DIFFERENT CONDITION

The above simulation is performed under certain assumptions. Now, the system performance is analyzed by changing some influence factors.

First, the quantity of LEO users is considered an influence factor. As we know, with more LEO users, more constraints should be considered, which means that except for the worst user existed, there may be a much worse user. If so, the beamhopping sequence and adaptive power will accordingly make a difference.

Simulations are performed by considering random distribution of multiple users around the center of the beams. The number of users in each beam is identical. Fig. 14 shows the variation of the SINR when 5 LEO users are placed in each beam. A comparison with Fig. 13 clearly shows that the SINR of the GEO users declines within a certain period of time.

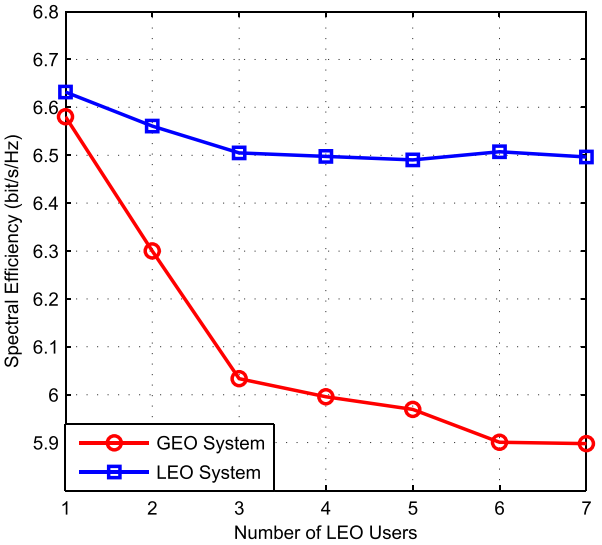


**FIGURE 15.** Spectral efficiency versus number of LEO user in each beam.

To analyze the detailed effect on the number of LEO users, the spectral efficiency is simulated. Fig. 15 shows the spectral efficiency of the GEO and LEO systems versus the number of LEO users in a beam. As shown in Fig. 15, the spectral efficiency of the GEO system almost reaches the efficiency of the LEO system when there is only one user in each beam. However, when the quantity increases, interference becomes stronger, which decreases the spectral

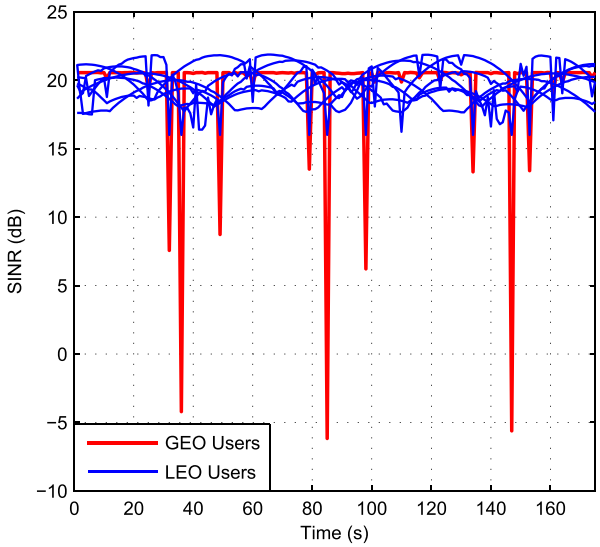


**FIGURE 16.** SINR of the users (satellite antenna diameter: 1.5 m).

efficiency for both systems. To maintain the normal operation of the primary system, the GEO system further decreases. Nevertheless, the rate of decrease tends to be steady when quantity reaches 3.

Second, the scenarios with different GEO beam sizes are analyzed. The beam size is changed using different antenna diameters, which also makes the antenna gain change, which is unfair to compare the effect for different beam sizes. Therefore, the *EIRP* of each beam is set to remain steady by adaptively adjusting the transmit power for all GEO beams. Fig. 16 shows the SINR of the GEO and LEO users when the antenna diameter is 1.5 m. A comparison with Fig. 13 shows that with a wider beam, the time interval between the strong interference increases. However, the spectral efficiency of both systems is not sensitive to the beam size as shown in Fig. 17 because the strong interference sustains for short

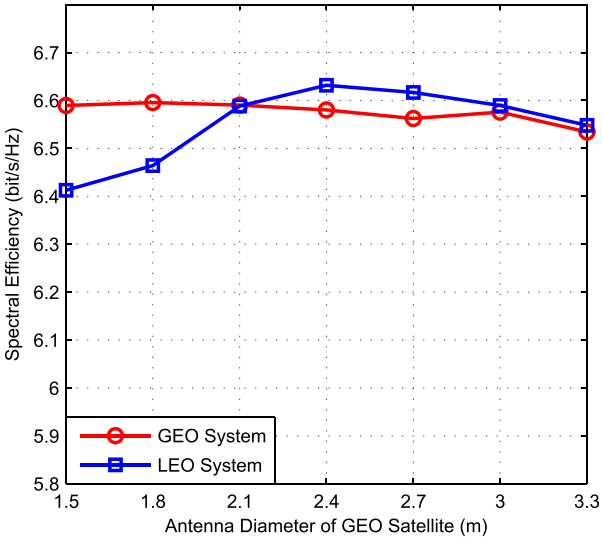


**FIGURE 17.** Spectral efficiency versus GEO beam size.

durations, and the beamhopping technique can mitigate most of the interference effect.

Finally, the scenarios at different latitudes are analyzed. Due to the smaller coverage area, each LEO satellite provides service to the area of the Earth beneath it, and compared with the GEO satellite, the beam of the LEO satellite only needs to be within a narrow range of angles relative to the nadir pointing direction. In addition, in this work the antennas of GEO and LEO users continue tracking their respective satellite. Therefore, the geometrical relationship between the satellites and users varies at different latitudes, as shown in Fig. 18.

Through geometric analysis, we get the relationship between the off-boresight angles and latitudes: the off-boresight angles of the desired transmitter $\theta_T$ for both GEO and LEO systems are always smaller than the angle corresponding to 3dB beamwidth, because the users are covered by the desired satellite beam; the off-boresight angles of the desired receiver are zero, because the antennas of GEO and LEO users point their respective satellite; the off-boresight angles of the receiver from interference link $\theta_R$ increase with the increase of latitude for both GEO and LEO systems.

According to the gain pattern of the user's antenna in Fig. 8, five-degree increase reduces the gain of interference signal by 36 dB and the interference rapidly decreases with an increasing angle. Conversely, the gains related to the desired signal are almost unchanged. Therefore, the off-boresight angle of the receiver from interference link $\theta_R$ plays a major role both for GEO and LEO systems. Specifically, it can be deduced that the intensity of the in-line interference decreases with increasing latitude based on (11).

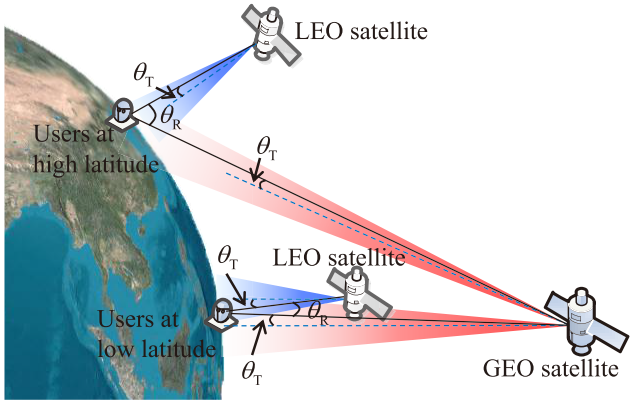


**FIGURE 18.** Geometrical relationship between the satellites and users at different latitudes.

The location of the user in No.1 beam is defined as the latitude of the scenario in the simulation, and the other users are still distributed around it. With the increase of the latitude, the LEO satellite's position changes as well, whereas only the pointing of GEO beam changes, as shown in Fig. 18. Fig. 19 shows the variation of the SINR when the location is at 30° northern latitude. The LEO satellite is in the polar orbit, and move gradually from high latitudes to low latitudes

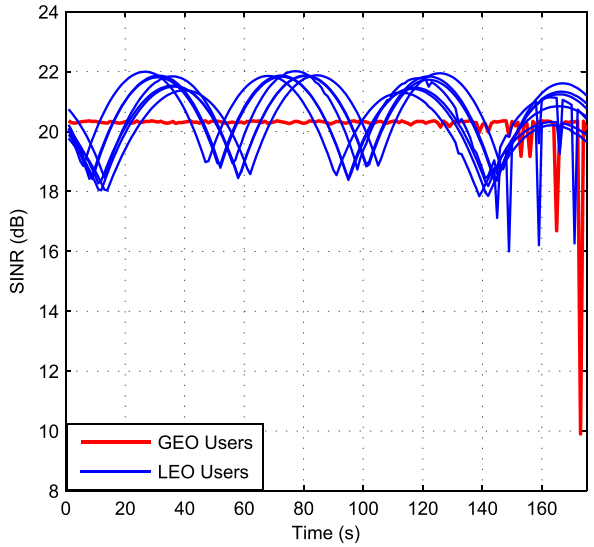


**FIGURE 19.** SINR of the users (scenario at 30° north latitude).

during the simulation. With the motion of LEO satellite, the $\theta_R$ of the interference link decreases. Thus, there is scarce interference at first due to the large $\theta_R$, and only weak interference arises at the end. Through further analysis, we find that when the scenario is at latitudes above 35°, the system is no longer affected by the interference during the entire passage of the LEO satellite.

It can be concluded that when located at high latitudes, the users would only potentially receive the interference: (i) very low-power signals from the far-out sidelobes of the satellite that are in the main beam of the user, and (ii) maximum power signals from the satellite that appear in the far-out sidelobes of the user. Nevertheless, both of them are weak. Therefore, both systems can share the same spectrum in harmony at high latitudes. In this work, the antenna of user is set to track the corresponding satellite in view of fixed broadband service. In practice, it may be assigned as needed, and the specific value of the latitude free from interference is related to coverage area of the LEO satellite, antenna pattern and antenna pointing.

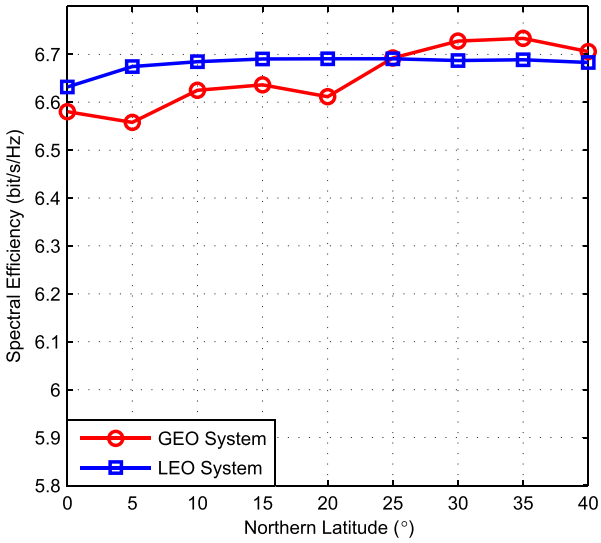


**FIGURE 20.** Spectral efficiency versus latitude.

The spectral efficiency of the networks at different northern latitudes is simulated as shown in Fig. 20. With the increase in latitude, the spectral efficiency increases. However, the increase soon saturates, particularly for the LEO satellite because of the protection mechanism for the LEO system. For the GEO satellite, the spectral efficiency slightly increases and decreases at some latitudes because the distance between the satellite and the user increases with the increase in latitude. Then, the free space propagation loss will increase. Eventually, the desired signal quality received by the users is reduced.

## V. CONCLUSION

This paper presents an interference analysis model in the time dimension for the coexistence of multiple satellite systems. A new cognitive network is proposed with LEO, which operates as the primary system, and GEO, which operates as the second system. During the passage of the LEO satellite, interference arises and affects both systems. Then, an algorithm with beamhopping and adaptive power control techniques is proposed for spectrum sharing. Because of the information exchange of satellite ephemeris between GEO and LEO systems, the GEO satellite can mitigate the interference. The simulation results demonstrate that the spectral efficiency of the GEO almost reaches that of the LEO, and the LEO system is well protected. Moreover, the spectrum-sharing method between GEO and LEO satellite systems can be widely used based on the analysis of the factors that affect the system performance.

## APPENDIX

Satellite Ephemeris Data and Parameter Definitions

- $a$ Semimajor axis
- $e$ Eccentricity
- $i_0$ Inclination angle
- $\Omega_0$ Longitude of the ascending node
- $\omega$ Argument of perigee
- $t_p$ Time past perigee
- $M_0$ Mean anomaly
- $\Omega_e = 7.29211585275553\text{e-}5$ rad/s Earth rotation rate
- $\psi_a$ Azimuth angle of beam direction
- $\psi_e$ Elevation angle of beam direction
- $a_0 = 6378.137$ km Radius of the Earth
- ${e_0}^2 = 0.00669438$ Elliptical eccentricity of the Earth
- $\varphi$ Geodetic latitude
- $\lambda$ Geodetic longitude
- $h_0$ Geodetic height

Computation of the ECEF Position Vector of a Satellite

(1) $n_0 = \sqrt{\mu/a^3}$ Mean motion $\mu = 398600.5 \times 10^9\ m^3/s^2$

(2) $t_k = t - t_{\mathrm{p}}$ Time from ephemeris epoch

(3) $M_k = M_0 + n_0 t_k$ Mean anomaly

(4) $E_k = M_k + e \sin E_k$ Eccentric anomaly

(5) $\sin f_k = \frac{\sqrt{1-e^2}\sin E_k}{1-e\cos E_k}$, $\cos f_k = \frac{\cos E_k - e}{1-e\cos E_k}$ True anomaly

(6) $u_k = f_k + \omega$ Argument of latitude

(7) $\Omega_k = \Omega_0 - \Omega_e\left(t_k - t_{\mathrm{p}}\right)$ Corrected longitude of node

(8) $r_k = a\left(1 - e\cos E_k\right)$ Orbital radius

(9) $x_k = r_k \cos u_k$ In-plane x position

(10) $y_k = r_k \sin u_k$ In-plane y position

(11) $$R_s = \begin{bmatrix} x_s \\ y_s \\ z_s \end{bmatrix} = \begin{bmatrix} x_k\cos\Omega_k - y_k\cos i_0 \sin\Omega_k \\ x_k\sin\Omega_k + y_k\cos i_0\cos\Omega_k \\ y_k \sin i_0 \end{bmatrix}$$

Computation of the ECEF Velocity Vector of a Satellite

(1) $\frac{dE_k}{dt} = n_0/(1 - e\cos E_k)$

(2) $\frac{du_k}{dt} = \sqrt{1+e/1-e}\left[\cos^2\left(\frac{f_k}{2}\right)/\cos^2\left(\frac{E_k}{2}\right)\right]\cdot\frac{dE_k}{dt}$

(3) $\frac{dr_k}{dt} = a\cdot e\cdot\sin(E_k)\cdot\frac{dE_k}{dt}$

(4) $\frac{dx_k}{dt} = \cos u_k\cdot\frac{dr_k}{dt} - r_k\sin u_k\cdot\frac{du_k}{dt}$

(5) $\frac{dy_k}{dt} = \sin u_k\cdot\frac{dr_k}{dt} + r_k\cos u_k\cdot\frac{du_k}{dt}$

(6) $$V_s = \begin{bmatrix} v_x \\ v_y \\ v_z \end{bmatrix} = \begin{bmatrix} \frac{dx_k}{dt}\cos\Omega_k - \frac{dy_k}{dt}\cos i_0\sin\Omega_k \\ \frac{dx_k}{dt}\sin\Omega_k + \frac{dy_k}{dt}\cos i_0\cos\Omega_k \\ \frac{dy_k}{dt}\sin i_0 \end{bmatrix}$$

Computation of the ECEF Position Vector of a User from Geodetic Coordinates

$$R_u = \begin{bmatrix} x_u \\ y_u \\ z_u \end{bmatrix} = \begin{bmatrix} \frac{a_0\cos\lambda}{\sqrt{1+(1-e_0^2)\tan^2\varphi}} + h_0\cos\lambda\cos\varphi \\ \frac{a_0\sin\lambda}{\sqrt{1+(1-e_0^2)\tan^2\varphi}} + h_0\sin\lambda\cos\varphi \\ \frac{a_0(1-e_0^2)\sin\varphi}{\sqrt{1-e_0^2\sin^2\varphi}} + h_0\sin\varphi \end{bmatrix}$$

Computation of the ECEF Vector for the Beam Direction

$$\cos(90^\circ - \psi_{\mathrm{e}}) = \frac{R_s\cdot(R_s - R_b)}{\|R_s\|\|R_s - R_b\|}$$

$$\cos\psi_{\mathrm{a}} = \frac{V_s\cdot(R_b - V_s)}{\|V_s\|\|R_b - V_s\|}$$

$$R_b = \begin{bmatrix} x_b \\ y_b \\ z_b \end{bmatrix} = \begin{bmatrix} x_b \\ y_b \\ 1 \end{bmatrix}$$

Computation of the Distance Between the Satellite and the User

$$d = \|R_s - R_u\|$$

Computation of the Off-boresight Angle Between the User and the Beam Direction

$$\phi = \arccos\frac{(R_u - R_s)\cdot(R_b - R_s)}{\|R_u - R_s\|\|R_b - R_s\|}$$

## REFERENCES

[1] A. H. Sanchez, T. Soares, and A. Wolahan, "Reliability aspects of mega-constellation satellites and their impact on the space debris environment," in *Proc. RAMS*, Jan. 2017, pp. 1–5.

[2] W. A. Hanson, "In their own words: OneWeb's Internet constellation as described in their FCC form 312 application," *New Space*, vol. 4, no. 3, pp. 153–167, 2016.

[3] *LeoSat Non-Geostationary Satellite System Attachment A: Technical Annex to Supplement Schedule S*. Accessed: Mar. 20, 2018. [Online]. Available: http://licensing.fcc.gov/myibfs/download.do?attachment_key=1158225

[4] A. Clegg and A. Weisshaar, "Future radio spectrum access [scanning the issue]," *Proc. IEEE*, vol. 102, no. 3, pp. 239–241, Mar. 2014.

[5] J. Mitola and G. Q. Maguire, Jr., "Cognitive radio: Making software radios more personal," *IEEE Pers. Commun.*, vol. 6, no. 4, pp. 13–18, Apr. 1999.

[6] M. Nitti, M. Murroni, M. Fadda, and L. Atzori, "Exploiting social Internet of things features in cognitive radio," *IEEE Access*, vol. 4, pp. 9204–9212, Dec. 2016.

[7] A. Gupta and E. R. K. Jha, "A survey of 5G network: Architecture and emerging technologies," *IEEE Access*, vol. 3, pp. 1206–1232, Jul. 2015.

[8] S. Ghahremani, R. H. Khokhar, R. M. Noor, A. Naebi, and J. Kheyrihassankandi, "On QoS routing in mobile WiMAX cognitive radio networks," in *Proc. Int. Conf. Comput. Commun. Eng. (ICCCE)*, Jul. 2012, pp. 467–471.

[9] S. Kumar and R. M. Hegde, "An efficient compartmental model for real-time node tracking over cognitive wireless sensor networks," *IEEE Trans. Signal Process.*, vol. 63, no. 7, pp. 1712–1725, Apr. 2015.

[10] P. Jacob, R. P. Sirigina, A. S. Madhukumar, and V. A. Prasad, "Cognitive radio for aeronautical communications: A survey," *IEEE Access*, vol. 4, pp. 3417–3443, May 2016.

[11] Y. Teng and M. Song, "Cross-layer optimization and protocol analysis for cognitive ad hoc communications," *IEEE Access*, vol. 5, pp. 18692–18706, Feb. 2017.

[12] S. K. Sharma, S. Chatzinotas, and B. Ottersten, "Cognitive radio techniques for satellite communication systems," in *Proc. IEEE 78th Veh. Technol. Conf. (VTC Fall)*, Sep. 2013, pp. 1–5.

[13] A. Vanelli-Coralli *et al.*, "Cognitive radio scenarios for satellite communications: The CoRaSat project," in *Cooperative and Cognitive Satellite Systems*. London, U.K.: Academic, 2015, ch. 10, pp. 303–336.

[14] M. Höyhtyä *et al.*, "Database-assisted spectrum sharing in satellite communications: A survey," *IEEE Access*, vol. 5, pp. 25322–25341, Dec. 2017.

[15] T. Yucek and H. Arslan, "A survey of spectrum sensing algorithms for cognitive radio applications," *IEEE Commun. Surveys Tuts.*, vol. 11, no. 1, pp. 116–130, 1st Quart., 2009.

[16] M. A. Clark and K. Psounis, "Equal interference power allocation for efficient shared spectrum resource scheduling," *IEEE Trans. Wireless Commun.*, vol. 16, no. 1, pp. 58–72, Jan. 2017.

[17] M. Jia, X. Liu, X. Gu, and Q. Guo, "Joint cooperative spectrum sensing and channel selection optimization for satellite communication systems based on cognitive radio," *Int. J. Satellite Commun.*, vol. 35, no. 2, pp. 139–150, Mar./Apr. 2017.

[18] S. K. Sharma, T. E. Bogale, S. Chatzinotas, B. Ottersten, L. B. Le, and X. Wang, "Cognitive radio techniques under practical imperfections: A survey," *IEEE Commun. Surveys Tuts.*, vol. 17, no. 4, pp. 1858–1884, 4th Quart., 2015.

[19] M. Höyhtyä, J. Kyröläinen, A. Hulkkonen, J. Ylitalo, and A. Roivainen, "Application of cognitive radio techniques to satellite communication," in *Proc. IEEE Int. Symp. Dyn. Spectr. Access Netw. (DYSPAN)*, Oct. 2012, pp. 540–551.

[20] C. Yuan, M. Lin, J. Ouyang, and Y. Bu, "Beamforming schemes for hybrid satellite-terrestrial cooperative networks," *AEU Int. J. Electron. Commun.*, vol. 69, no. 8, pp. 1118–1125, Aug. 2015.

[21] S. K. Sharma, S. Chatzinotas, and B. Ottersten, "Transmit beamforming for spectral coexistence of satellite and terrestrial networks," in *Proc. CrownCom*, Jul. 2013, pp. 275–281.

[22] L. F. Abdulrazak, "FSS shielding and antenna discrimination effect on interference mitigation techniques," in *Proc. CSSCC*, Mar. 2014, pp. 248–253.

[23] S. Mangold, A. Jarosch, and C. Monney, "Operator assisted cognitive radio and dynamic spectrum assignment with dual beacons—Detailed evaluation," in *Proc. Comsware*, Jan. 2006, pp. 1–6.

[24] A. Rabbachin, T. Q. S. Quek, H. Shin, and M. Z. Win, "Cognitive network interference," *IEEE J. Sel. Areas Commun.*, vol. 29, no. 2, pp. 480–493, Feb. 2011.

[25] S. K. Sharma, S. Chatzinotas, and B. Ottersten, "Interference alignment for spectral coexistence of heterogeneous networks," *EURASIP J. Wireless Commun. Netw.*, vol. 2013, no. 1, p. 46, 2013.

[26] S. Chatzinotas, S. K. Sharma, and B. Ottersten, "Frequency packing for interference alignment-based cognitive dual satellite systems," in *Proc. IEEE Veh. Technol. Conf.*, Sep. 2013, pp. 1–7.

[27] D. Christopoulos, S. Chatzinotas, and B. Ottersten, "User scheduling for coordinated dual satellite systems with linear precoding," in *Proc. IEEE Int. Conf. Commun.*, Jun. 2013, pp. 4498–4503.

[28] E. Lagunas, S. Maleki, S. Chatzinotas, M. Soltanalian, A. I. Pérez-Neira, and B. Oftersten, "Power and rate allocation in cognitive satellite uplink networks," in *Proc. IEEE Int. Conf. Commun. (ICC)*, May 2016, pp. 1–6.

[29] S. K. Sharma, S. Chatzinotas, and B. Ottersten, "In-line interference mitigation techniques for spectral coexistence of GEO and NGEO satellites," *Int. J. Satellite Commun. Netw.*, vol. 34, no. 1, pp. 11–39, 2016.

[30] S. Vassaki, M. I. Poulakis, and A. D. Panagopoulos, "Optimal iSINR-based power control for cognitive satellite terrestrial networks," *Trans. Emerg. Telecommun. Technol.*, vol. 28, no. 2, p. e2945, Feb. 2017.

[31] S. K. Sharma, S. Chatzinotas, and B. Ottersten, "Cognitive beamhopping for spectral coexistence of multibeam satellites," *Int. J. Satellite Commun. Netw.*, vol. 33, no. 1, pp. 69–91, 2015.

[32] J. Anzalchi *et al.*, "Beam hopping in multi-beam broadband satellite systems: System simulation and performance comparison with non-hopped systems," in *Proc. 5th Adv. Satellite Multimedia Syst. Conf./11th Signal Process. Space Commun. Workshop*, Sep. 2010, pp. 248–255.

[33] R. Alegre-Godoy and M. A. Vazquez-Castro, "Spatial diversity with network coding for on/off satellite channels," *IEEE Commun. Lett.*, vol. 17, no. 8, pp. 1612–1615, Aug. 2013.

[34] R. Suffritti *et al.*, "Cognitive hybrid satellite-terrestrial systems," in *Proc. 4th Int. Conf. Cognit. Radio Adv. Spectr. Manage. (CogART)*, Oct. 2011, Art. no. 64.

[35] S. Vassaki, M. I. Poulakis, A. D. Panagopoulos, and P. Constantinou, "Power allocation in cognitive satellite terrestrial networks with QoS constraints," *IEEE Commun. Lett.*, vol. 17, no. 7, pp. 1344–1347, Jul. 2013.

[36] S. Kandeepan, L. De Nardis, M. G. Di Benedetto, A. Guidotti, and G. E. Corazza, "Cognitive satellite terrestrial radios," in *Proc. IEEE Global Telecommun. Conf. (GLOBECOM)*, Dec. 2010, pp. 1–6.

[37] S. K. Sharma, S. Chatzinotas, and B. Ottersten, "Spectrum sensing in dual polarized fading channels for cognitive SatComs," in *Proc. IEEE Global Telecommun. Conf. (GLOBECOM)*, Dec. 2012, pp. 3419–3424.

[38] P. Ren, Y. Wang, Q. Du, and J. Xu, "A survey on dynamic spectrum access protocols for distributed cognitive wireless networks," *EURASIP J. Wireless Commun. Netw.*, vol. 2012, no. 1, p. 60, 2012.

[39] N. Devroye, P. Mitran, and V. Tarokh, "Achievable rates in cognitive radio channels," *IEEE Trans. Inf. Theory*, vol. 52, no. 5, pp. 1813–1827, May 2006.

[40] M. A. Vazquez-Castro, D. Belay-Zelek, and A. Curieses-Guerrero, "Availability of systems based on satellites with spatial diversity and HAPS," *Electron. Lett.*, vol. 38, no. 6, pp. 286–288, Mar. 2002.

[41] J. M. P. Fortes, R. Sampaio-Neto, and J. E. A. Maldonado, "An analytical method for assessing interference in interference environments involving NGSO satellite networks," *Int. J. Satellite Commun. Netw.*, vol. 17, no. 6, pp. 399–419, Nov./Dec. 1999.

[42] C.-S. Park, C.-G. Kang, Y.-S. Choi, and C.-H. Oh, "Interference analysis of geostationary satellite networks in the presence of moving non-geostationary satellites," in *Proc. ICTS*, Aug. 2010, pp. 1–5.

[43] *Method to Enhance Sharing Between Non-GSO FSS Systems (Except MSS Feeder Links) in the Frequency Bands Between 10-30 GHz*, document ITU-R Rec. S.1431, 2000.

[44] *O3b: A Breakthrough Technology for Broadband Satellite Service*. Accessed: Mar. 20, 2018. [Online]. Available: http://www.itso.int/images/stories/GSR-12/jreadpresentation.pdf

[45] *Radio Regulations*, Int. Telecommun. Union, Geneva, Switzerland, 2015.

[46] G. Maral and M. Bousquet, "Satellite communications systems: Systems, techniques and technology," *Electron. Radio Eng. J. Inst.*, vol. 56, nos. 8–9, p. 742, 2011.

[47] E. Kaplan and C. Hegarty, "Fundamentals of satellite navigation," in *Understanding GPS: Principles and Applications*, 2nd ed. London, U.K.: Artech House, 2005, ch. 2, sec. 3, pp. 34–43.

[48] M. A. Dlaz, N. Courville, C. Mosquera, G. Liva, and G. E. Corazza, "Non-linear interference mitigation for broadband multimedia satellite systems," in *Proc. Int. Workshop Satellite Space Commun. (IWSSC)*, Sep. 2007, pp. 61–65.

[49] C. J. Wang, "Structural properties of a low Earth orbit satellite constellation—The Walker delta network," in *Proc. Conf. Rec. Commun. Move Military Commun. Conf. (MILCOM)*, vol. 3. Oct. 1993, pp. 968–972.

[50] P. Angeletti, D. F. Prim, and R. Rinaldo, "Beam hopping in multi-beam broadband satellite systems: System performance and payload architecture analysis," in *Proc. 24th AIAA Int. Commun. Satellite Syst. Conf. (ICSSC)*, vol. 1. Jul. 2006, pp. 596–605.

[51] H. Bischl *et al.*, "Adaptive coding and modulation for satellite broadband networks: From theory to practice," *Int. J. Satell. Commun. Netw.*, vol. 28, no. 2, pp. 59–111, 2010.

[52] C. Popper, M. Strasser, and S. Capkun, "Anti-jamming broadcast communication using uncoordinated spread spectrum techniques," *IEEE J. Sel. Areas Commun.*, vol. 28, no. 5, pp. 703–715, Jun. 2010.


**CHUANG WANG** was born in Dangtu County, China. He received the B.S. and M.S. degrees from the College of Communications Engineering, PLA University of Science and Technology, Nanjing, in 2016. He is currently pursuing the Ph.D. degree in information and communication engineering with the Army Engineering University of PLA, China. His research interests include satellite communication, constellation design, and space information network.

**DONGMING BIAN** received the Ph.D. degree from the PLA University of Science and Technology, Nanjing, China, in 2004. He is currently a Professor with the Nanjing Institute of Communication Engineering, PLA University of Science and Technology. His research interests include wireless communications, satellite communications, and deep space communications.

**SHENGCHAO SHI** was born in Jimo County, China, in 1988. He received the B.S. and M.S. degrees from the College of Communications Engineering, PLA University of Science and Technology, Nanjing, in 2014. He is currently pursuing the Ph.D. degree in information and communication engineering with the Army Engineering University of PLA, China. His research interests include satellite communication and cognitive satellite network.

**JUN XU** was born in Yongcheng County, China. He received the B.S. degree from the College of Information Science and Engineering, Southeast University, Nanjing, in 2016. He is currently pursuing the M.S. degree in information and communication engineering with the Army Engineering University of PLA, China. His research interests include satellite communication and constellation design.

**GENGXIN ZHANG** received the Ph.D. degree from the Nanjing Institute of Communication Engineering, Nanjing, China, in 1993. He is currently a Professor with the Nanjing Institute of Communication Engineering, PLA University of Science and Technology, China. His research interests include design of communication systems and satellite and deep space communications.